Spectroscopic Properties of the Metalloregulatory Cd(II) and Pb(II) Sites of *S. aureus* pI258 CadC†

Laura S. Busenlehner,‡ Nathaniel J. Cosper,§ Robert A. Scott,§ Barry P. Rosen,|| Marco D. Wong,|| and David P. Giedroc*,‡

Department of Biochemistry and Biophysics, Center for Advanced Biomolecular Research, Texas A&M University, College Station, Texas 77843-2128, Department of Chemistry, University of Georgia, Athens, Georgia 30602-2556, and Department of Biochemistry and Molecular Biology, Wayne State University School of Medicine, Detroit, Michigan 48201

Received January 2, 2001; Revised Manuscript Received February 13, 2001

ABSTRACT: *Staphylococcus aureus* pI258 CadC is an extrachromosomally encoded metalloregulatory repressor protein from the ArsR superfamily which negatively regulates the expression of the *cad* operon in a metal-dependent fashion. The metalloregulatory hypothesis holds that direct binding of thiophilic divalent cations including Cd(II), Pb(II), and Zn(II) by CadC allosterically regulates the DNA binding activity of CadC to the *cad* operator/promoter (O/P). This report presents a detailed characterization of the metal binding and DNA binding properties of wild-type CadC. The results of analytical ultracentrifugation experiments suggest that both apo- and Cd_1-CadC are stable or weakly dissociable homodimers characterized by a $K_{dimer} = 3.0 \times 10^6$ M^{-1} (pH 7.0, 0.20 M NaCl, 25.0 °C) with little detectable effect of Cd(II) on the dimerization equilibrium. As determined by optical spectroscopy, the stoichiometry of Cd(II) and Pb(II) binding is ≈0.7−0.8 mol/mol of wild-type CadC monomer. Chelator (EDTA) competition binding isotherms reveal that Cd(II) binds very tightly, with $K_{Cd} = 4.3$ (±1.8) $\times 10^{12}$ M^{-1}. The results of UV−Vis and X-ray absorption spectroscopy of the Cd_1 complex are consistent with a tetrathiolate (S_4) complex formed by four cysteine ligands. The ^{113}Cd NMR spectrum reveals a single resonance of $\delta =$ 622 ppm, consistent with an S_3(N,O) or unusual upfield-shifted S_4 complex. The Pb(II) complex reveals two prominent absorption bands at 350 nm ($\epsilon = 4000$ M^{-1} cm^{-1}) and 250 nm ($\epsilon = 41\,000$ M^{-1} cm^{-1}), spectral properties consistent with three or four thiolate ligands to the Pb(II) ion. The change in the anisotropy of a fluorescein-labeled oligonucleotide containing the *cad* O/P upon binding CadC and analyzed using a dissociable CadC dimer binding model reveals that apo-CadC forms a high-affinity complex [$K_a = (1.1 \pm 0.3) \times 10^9$ M^{-1}; pH 7.0, 0.40 M NaCl, 25 °C], the affinity of which is reduced ≈300-fold upon the binding of a single molar equivalent of Cd(II) or Pb(II). The implications of these findings on the mechanism of metalloregulation are discussed.

Metal-responsive control of the expression of genes involved in metal ion homeostasis allows organisms to tightly regulate the free concentrations of essential metal ions, while efficiently removing toxic or nonessential metals (*1, 2*). Bacteria have evolved detoxification systems for a variety of metals including arsenic, antimony, zinc, copper, cadmium, lead, and mercury (*3, 4*). These systems are generally composed of a metal-specific regulatory protein and one or more detoxification proteins, such as membrane P-type ATPase metal efflux pumps, metal sequestering proteins, or metal reductases (*3*−*6*).

One well-studied family of metalloregulatory transcription factors, the ArsR family, is known to negatively regulate the expression of genes encoding metal efflux pumps or metal chelators (*1, 5, 7*). Included in this family is *Staphylococcus aureus* pI258 CadC which negatively regulates transcription of the *cad* operon. The *cad* operon is composed of two genes which encode CadC and CadA, the P-type ATPase efflux pump that is specific for Pb(II), Cd(II), and Zn(II) (*8, 9*). *CadA* transcription is repressed in the absence of Pb(II), Cd(II), Zn(II), or Bi(III) in the growth media and is derepressed by an increase in the concentrations of these metals (*8*−*10*). In addition, in vitro transcription experiments using *E. coli* RNA polymerase revealed that cadmium relieved transcriptional repression by CadC at the *cad* operator/promoter (*11*). Gel retardation experiments with CadC suggest that cadmium and lead induce the partial dissociation of the repressor from the *cad* operator/promoter, and DNase I footprinting mapped this specific interaction between the −10 element and the transcriptional start site (*11*). Finally, using an in vitro restriction enzyme protection assay, we have demonstrated that incubation of CadC with lead, cadmium, or zinc results in an increase in accessibility of the *cad* O/P (*10*).

The X-ray crystallographic structure of *Synechococcus* PCC7942 SmtB, a member of the ArsR family, has been

† This work was supported by NIH Grants GM42569 (to D.P.G.), GM42025 (R.A.S.), and AI45428 (B.P.R.) and by the Robert A. Welch Foundation (A-1295 to D.P.G.).

* To whom correspondence should be addressed. E-mail: giedroc@tamu.edu, Telephone: 979-845-4231, Fax: 979-862-4718.

‡ Texas A&M University.

§ University of Georgia.

|| Wayne State University School of Medicine.

10.1021/bi010006g CCC: $20.00
Published on Web 03/16/2001

determined (*12*). SmtB is a zinc-responsive transcriptional repressor of the *smt* operon which encodes a class II metallothionein (SmtA) that functions to sequester zinc (*13, 14*). The structure of metal-free SmtB revealed a dimeric, largely α-helical protein that has a 2-fold axis of symmetry. Mercuric acetate soaks of the apo-SmtB crystals were interpreted to suggest that each monomer binds two Zn(II) ions, one at the dimer interface involving the C-terminal α5 helix, and another near the putative metal binding motif ELCV(G/C)D (*12*). We have recently shown using direct measurements that each SmtB monomer binds only 1 mol equiv of Zn(II) or Co(II) and that one or two cysteine thiolates are involved in direct coordination of this metal (*15*). *S. aureus* pI258 CadC is 29% identical to SmtB and contains the conserved $E^{56}L\mathbf{C}V\mathbf{C}D^{61}$ motif; note, however, that Cys60 is a Gly residue in SmtB (*5*). In addition, there are three additional cysteines, two (Cys7 and Cys11) at the N-terminal region, one of which (Cys7) is conserved in SmtB but which is not observed crystallographically, and another, Cys52, which is just N-terminal to the putative metal binding motif. Recent studies demonstrate that Cys7, Cys58, and Cys60 are required for sensing of lead, cadmium, and zinc by CadC, both in vivo and in vitro (*10*).

In this report, we present direct evidence showing that CadC binds Cd(II) and Pb(II), both of which regulate the expression of the *cad* operon in vivo (*8*−*10*). The results of UV−Vis and X-ray spectroscopic (EXAFS)[1] measurements are consistent with a tetrathiolate Cd(II) site in CadC formed by four cysteine thiolate ligands. Based on EDTA competition experiments, the Cd(II) ion is bound tightly [$K_{Cd} = 4.3 (\pm 1.8) \times 10^{12}$ M^{-1}]. ^{113}Cd NMR spectroscopy exhibits a single resonance at $\delta = 622$ ppm which is within the range of an unusual upfield-shifted S_4 site or an S_3(N,O) site (*16*). The Pb(II) UV−Vis spectrum is consistent with a Pb(II) site composed of three or four cysteine thiolate ligands. Fluorescence anisotropy experiments with a fluorescein-labeled *cad* O/P oligonucleotide reveal that both $Cd(II)_1$ and $Pb(II)_1$ CadC have reduced DNA binding affinities (≈300-fold decrease) compared to apo-CadC. The implications of these findings on the mechanism of metalloregulation by CadC are discussed.

MATERIALS AND METHODS

Chemicals.[1] All buffers were prepared using Milli-Q deionized water. MES and Bis-Tris buffer salts, ammonium sulfate, and 5,5′-dithiobis(2-nitrobenzoic acid) were purchased from Sigma. Chromatography materials were obtained from Pharmacia Biotech. Ultrapure cadmium(II) chloride and lead(II) chloride were acquired from Johnson Matthey. d^{18} HEPES and D_2O were obtained from Cambridge Isotopes.

Construction of CadC Overexpression Plasmids. Two different bacterial overexpression plasmids, pMW1 (Rosen lab) and pET-CadC (Giedroc lab), were used as the source of recombinant CadC. The construction of plasmid pMW1 has been described (*10*). For construction of plasmid pET-CadC, a CadC−GST fusion plasmid, *pSJL302*, generously provided by Dr. Simon Silver at the University of Illinois at Chicago, was used as the template for polymerase chain reaction (PCR). PCR primers flanking the CadC gene were designed with incorporated *Nco*I and *Bam*HI restriction endonuclease sites to permit subcloning of the purified PCR product directly into the *Nco*I/*Bam*HI-restricted pET-3d expression plasmid (Promega) using standard cloning techniques to create pET-CadC (*16*). The integrities of both pET-CadC and pMW1 were verified by dideoxy sequencing.

Purification of CadC. For production of CadC from pET-CadC, the plasmid was transformed into *E. coli* BL21(DE3)/*pLysS* and grown on a 1.5% LB agar plate containing 0.1 mg/mL ampicillin and 34 μg/mL chloramphenicol at 37 °C. A single colony was used for a 200 mL overnight seed culture that was used to inoculate 9 L of LB containing ampicillin and chloramphenicol. The cells were grown at 37 °C with stirring (300 rpm) to an OD of 0.7−0.8 at 600 nm in a New Brunswick Scientific Series 25 incubator/shaker. Addition of IPTG to a final concentration of 800 μM induced the expression of CadC. Cells were harvested by centrifugation and yielded 25−30 g of wet cell paste that was used immediately for purification.

Purification of CadC from *E. coli* strain BL21(DE3)/pMW1 has been described (*10*). CadC from plasmid pET-CadC was purified by a variation of a procedure described (*15*). The freshly harvested cell paste was suspended in 200−250 mL of Buffer B (25 mM MES, 4 mM DTT, 1 mM EDTA, pH 6.0) containing 1 mL of 0.10 M PMSF and lysed by sonication using a Fisher Scientific model 550 sonic dismembrator. The cellular lysate was centrifuged at 8000 rpm for 30 min at 4 °C. The supernatant was collected and subjected to protein and nucleic acid precipitation using 10% polyethylenimine (0.015 v/v) at pH 6.0. After stirring for 2 h at 4 °C, the solution was centrifuged at 8000 rpm for 30 min at 4 °C. The supernatant was decanted, and the precipitate was resuspended in Buffer B containing 0.50 M NaCl to extract the protein. After 8 h of stirring, the extraction solution was centrifuged at 8000 rpm for 30 min. The protein in the supernatant was precipitated by the addition of $(NH_4)_2SO_4$ to 60% saturation with stirring for 2 h. After centrifugation at 8000 rpm for 30 min, the precipitated protein was dissolved in Buffer B so that the concentration of salt was 0.25 M (usually 200 mL). This solution was loaded onto a 60 mL SP Fast Flow gravity column equilibrated with Buffer B containing 0.25 M NaCl. After the sample was loaded, the column was washed with 60 mL of Buffer B with 0.25 M NaCl. The protein was then eluted using a 150 mL linear gradient of 0.25−1.0 M NaCl in Buffer B. CadC eluted at approximately 0.45 M NaCl. Fractions containing CadC were combined and concentrated to 5 mL using a 50 mL Amicon concentrator with a YM10 membrane. The sample was loaded onto a 100 mL Superdex 75 size-exclusion column equilibrated with Buffer B containing 0.45 M NaCl at a flow rate of 0.3 mL/min. CadC was eluted from the column with the same buffer at 0.3 mL/min. Fractions containing CadC were combined and reduced by the addition of 50 mM DTT at 30 °C for 2 h. The reduced CadC protein was dialyzed against 3 L of Buffer S (50 mM MES, 0.40 M NaCl, pH 7.0) in an anaerobic Vacuum Atmospheres glovebox with changes every 4 h for a total of

[1] Abbreviations: Bis-Tris, bis(2-hydroxyethyl)iminotris(hydroxymethyl)methane; DTNB, 5,5′-dithiobis(2-nitrobenzoic acid); EDTA, ethylenediaminetetracetic acid; EXAFS, extended X-ray absorption fine structure; HEPES, *N*-(2-hydroxyethyl)piperazine-*N*′-2-ethanesulfonic acid; IPTG, isopropyl β-D-thiogalactopyranoside; MES, 2-(*N*-morpholino)ethanesulfonic acid; PMSF, phenylmethylsulfonyl chloride; Tris, tris(hydroxymethyl)aminomethane; XAS, X-ray absorption spectroscopy.

12 h at room temperature. Inspection of overloaded Coomassie-stained Tricine−SDS gels was used to estimate the purity to be ≥95%. MALDI-TOF mass spectrometry reveals a mass of 13 787 daltons (13 779 daltons expected). The concentration of purified CadC was determined using the calculated molar extinction coefficient at 280 nm of 6585 M^{-1} cm^{-1} (*18*). Purified CadC was stored at −80 °C in an anaerobic environment in small aliquots.

Atomic Absorption Spectroscopy. The Zn(II) and Cd(II) content of CadC was determined using a Perkin-Elmer AAnalyst 700 atomic absorption spectrophotometer in flame mode using hollow cathode lamps specific for each metal (*19*). Zn(II) was detected at 213.9 nm (slit = 0.7 nm), and Cd(II) was detected at 228.8 nm (slit = 0.7 nm). The metal content of purified "metal-free" CadC was found to be 0.02 mol of Zn(II) and 0.03 mol of Cd(II) per mole of CadC monomer, at or near the limit of detection. The Cd(II) titrant concentrations for optical absorption were measured as described above. For the determination of the concentration of Pb(II) used for titrant stocks, Pb(II) was detected at 283.3 nm (slit = 0.7 nm).

Free Thiol Quantification. A standard DTNB colorimetric assay was used to determine the number of reduced thiols in CadC (*19*). A 25 μM aliquot of CadC was added to 400 μL of Buffer S containing 45 μL of 2.5 mM DTNB solution. The reaction was allowed to go to completion (30 min) in an anaerobic environment. The molar concentration of thiolate anion was quantified at 412 nm (ϵ = 13 600 M^{-1} cm^{-1}) after subtraction of the absorbance of buffer with DTNB. The calculated number of free thiols in CadC was determined to be 3.7 ± 0.2 free thiols per monomer (expected number is 5). We have confirmed the presence of a CadC disulfide cross-linked dimer, in addition to the monomer on denaturing SDS−PAGE gels. Both bands were subjected to automated Edman N-terminal sequencing using a Hewlett-Packard G1000A Automated Protein Sequencer and unambiguously gave the same amino acid residue sequence (MEKKNTXE; X = cysteine).

Analytical Sedimentation Equilibrium Ultracentrifugation. All experiments were run using a Beckman Optima XL-A analytical ultracentrifuge set to a speed of 35 000 rpm (89180*g* at the cell center) at 25.0 °C. Apo-CadC samples (10−40 μM) were prepared by dilution into 5 mM MES, 0.20 M NaCl, 2 mM DTT, 1 mM EDTA, pH 7.0. Cd(II)-CadC was prepared by addition of 1 molar equiv of Cd(II) to the apoprotein followed by dilution into 5 mM MES, 0.20 M NaCl, pH 7.0. The cells were assembled and loaded with CadC in an anaerobic environment. Sedimentation equilibrium data were evaluated using Microcal Origin, a nonlinear least-squares fitting program. The partial specific volume (ν) was calculated to be 0.724 mL/g, and the solvent density (ρ) was 1.006 g/mL. Model 1 fits the data to a single, ideal species using the equation:

$$A_r = A_0 \exp[H{\cdot}M(x^2 - x_0^2)] + E$$

where A_r = absorbance at radius x, A_0 = absorbance at the reference radius x_0, M = molecular weight, H = constant $(1 - \nu\rho)\omega^2/2RT$, and E = baseline offset. Model 2 fits the data to a self-association model of a single ideal species, assuming a monomer−dimer equilibrium characterized by the association constant K_a:

$$A_{r,\text{total}} = A_0 \exp[H{\cdot}M(x^2 - x_0^2)] + (A_0)^{n2}{\cdot}K_a \exp[H{\cdot}M{\cdot}n_2(x^2 - x_0^2)] + E$$

where M = monomer molecular weight, n_2 = stoichiometry (number of monomers), and K_a = association constant for the monomer−dimer equilibrium. The association constant was converted from absorbance to units of M^{-1} using the extinction coefficient ϵ_{280} = 6585 M^{-1} cm^{-1} and a path length l = 1.2 cm.

Cd(II) and Pb(II) Binding Experiments. All metal binding experiments were carried out anaerobically at ambient temperature (22 °C) using a Hewlett-Packard model 8452A spectrophotometer. For Cd(II) titrations, apo-CadC (0.8 mL of 15−45 μM) was diluted with buffer (5 mM MES, 0.20 M NaCl, pH 7.0) and loaded into an anaerobic cuvette fitted with an adjustable-volume Hamilton gastight syringe loaded with 250 μL of Cd(II) titrant prior to removal from the anaerobic glovebox. Optical spectra of apo-CadC and of the protein after each addition of a known aliquot (5−20 μL) of Cd(II) titrant were collected from 190 to 1100 nm. Corrected spectra were obtained by subtraction of the apo-CadC spectrum from each metal-addition spectrum and by correction for dilution. The binding isotherms were fit to a 1:1 binding model linked to the monomer−dimer equilibrium using DynaFit (*20*) to obtain the lower limit for K_{Cd}. Pb(II) titrations of apo-CadC (30−60 μM) were as described for Cd(II) except that the buffer used was 10 mM Bis-Tris, 0.20 M NaCl, pH 7.0. Bis-Tris is a weakly chelating buffer that is used to prevent excess Pb(II) ions from forming the insoluble precipitate $Pb(II)(OH)_2$ (*21*).

Cd(II) competition experiments with EDTA to determine K_{Cd} were performed as above except that excess EDTA was present to buffer low concentrations of free Cd(II). Each titration point was allowed to equilibrate 2−4 min. The stability constant (K') of the Cd(II)−EDTA complex was calculated to be 3.2 × 10^{12} M^{-1} under these solution conditions (*22, 23*), and the data were fit with DynaFit (*20*) using a two-site model linked to the monomer−dimer equilibrium where K_{dimer} = 3 × 10^6 M^{-1}.

Cd(II) X-ray Absorption Spectroscopy. XAS samples were prepared by the addition of 0.9 mol equiv of Cd(II) to apo-CadC in 50 mM MES, 0.40 M NaCl, 20% glycerol, pH 7.0, in an anaerobic environment. These samples were loaded into polycarbonate XAS cuvettes, immediately frozen in liquid N_2. XAS data were collected at Stanford Synchrotron Radiation Laboratory (SSRL) with the SPEAR storage ring operating at 3.0 GeV (Table 1). EXAFS analysis was performed with EXAFSPAK software (courtesy of G. N. George; www-ssrl.slac.stanford.edu/exafspak.html) according to standard procedures (*15, 24*).

^{113}Cd NMR Spectroscopy. The ^{113}Cd NMR spectrum of CadC was recorded using a Varian Unity 500 spectrometer (110.9 MHz for ^{113}Cd) equipped with a broad-band tunable probe that accommodates 5 mm (o.d.) NMR tubes. Chemical shifts are reported relative to 0.10 M $Cd(ClO_4)_2$ measured in 5 mM d^{18} HEPES, 10% D_2O, pH 7.0. The protein sample was prepared by addition of 1 molar equiv of $^{113}CdCl_2$ to apo-CadC that was dialyzed against a deuterated HEPES buffer (5 mM d^{18} HEPES, 0.35 M NaCl, 10% D_2O, pH 7.0) in the anaerobic glovebox for 4 h at ambient temperature.

Table 1: X-ray Absorption Spectroscopic Data Collection

	Cd EXAFS
SR facility	SSRL
beamline	7-3
current in storage ring, mA	50−100
monochromator crystal	Si[220]
detection method	fluorescence
detector type	solid-state array[a]
scan length, min	25
scans in average	8
temperature, K	10
energy standard	Cd foil, first inflection
energy calibration, E_0, eV	
preedge background	
energy range, eV	26390−26675
Gaussian center, eV	23172
width, eV	750
spline background	
energy range, eV	26720−26986 (4)
(polynomial order)	26986−27253 (4)
	27253−27520 (4)

[a] The 13-element Ge solid-state X-ray fluorescence detector at SSRL is provided by the NIH Biotechnology Research Resource.

The final concentration of ^{113}Cd(II)-bound CadC determined by optical spectroscopy was 0.96 mM.

Fluorescence Anisotropy. All fluorescence anisotropy experiments were carried out with an SLM 4800 spectrofluorometer operating in the steady-state mode fitted with Glan-Thompson polarizers in the L format (*25*). The 34-mer, double-stranded *cad* O/P oligonucleotide (Operon Technologies) used was fluorescein-labeled on one 5′-end with the sequence given below.

F-5′-ATAATACACTCAAATAAATATTTGAATGA-AGATG-3′

3′-TATTATGTGAGTTTATTTATAAACTTACTTC-TAC-5′

Apo-, Cd_1-, or Pb_1- CadC was titrated into 1.7 mL of 20 nM *cad* O/P at 25 °C. The buffer used for the apo-CadC titration was 5 mM MES, 0.40 M NaCl, 1 mM DTT, 50 μM EDTA, pH 7.0 (for comparison with the Cd-CadC titration), or 10 mM Bis-Tris, 0.40 M NaCl, 1 mM DTT, 50 μM EDTA, pH 7.0 (for comparison with the Pb-CadC titration). For the Cd_1-CadC titration of *cad* O/P, 1 mol equiv of Cd(II) was added to apo-CadC anaerobically. The buffer used for the titration was 5 mM MES, 0.40 M NaCl, 1 mM DTT, pH 7.0. The Pb_1-CadC titration was like that for Cd_1-CadC except the buffer used was 10 mM Bis-Tris, 0.40 M NaCl, 1 mM DTT, pH 7.0.

Anisotropy data were fit using the program DynaFit (*20*) to a dissociable dimer model with a 1:1 binding stoichiometry (CadC dimer to *cad* O/P oligonucleotide) linked to a monomer−dimer equilibrium. The binding isotherms (raw r_{obs} vs $[CadC]_{total}$) were fit using a fixed dimerization constant, $K_{dimer} = 3 \times 10^6$ M^{-1}, based on sedimentation equilibrium ultracentrifugation experiments.

RESULTS

Characterization of Purified CadC. CadC was purified to near-homogeneity employing a procedure modeled after that used previously for *Synechococcus* SmtB (*15*) using a combination of ammonium sulfate precipitation, followed by cation exchange chromatography and gel filtration at pH 6.0 (see Materials and Methods). The protein is nearly homogeneous as revealed by an overloaded SDS−PAGE gel (Figure 1), with the exception of a minor contaminant that runs at a position essentially twice the expected molecular weight for the CadC monomer on these reducing, denaturing gels and comigrates with authentic CadC through all steps of the purification and immunoblots with anti-CadC serum (*10*). Both proteins were subjected to N-terminal sequencing and shown to have identical N-terminal sequences through 8 cycles, MEKKNTXE, which matches the expected N-terminal sequence of authentic CadC, if X = Cys7. No other N-terminal sequences were cleanly visible in these samples. The simplest interpretation of this result is that a fraction of the wild-type CadC exists as an irreversibly cross-linked dimer, which is refractory to reduction with excess reducing agent at elevated temperature. The fact that the number of reduced Cys residues per CadC monomer is consistently less than the 5 expected, and averages ≈3.7 Cys among multiple preparations of protein, is consistent with these species representing a disulfide cross-linked dimer. MALDI-TOF mass spectrometry data[2] show that a fraction of the CadC molecules, as isolated, contain an intermolecular disulfide bond between Cys58 in the putative metal binding sequence, $E^{56}LCVCD^{61}$, of one subunit and Cys7 or Cys11 of another subunit.

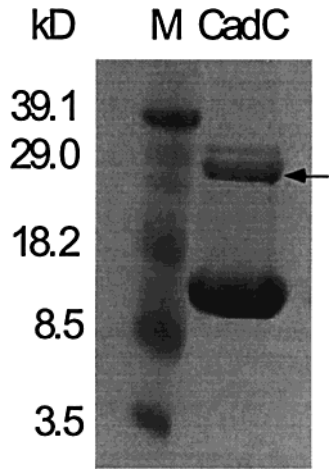

FIGURE 1: SDS−polyacrylamide gel electrophoresis of purified CadC. Lane 1, molecular mass markers (BioRad Kaleidoscope polypeptide standards). Lane 2, 30 μL of 200 μM purified CadC. The arrow identifies the protein band that was excised from the gel and subjected to N-terminal sequencing. Samples were heated at 95 °C for 5 min in 30 mM β-mercaptoethanol prior to being loaded on a Novex precast 16% Tris−Tricine SDS−PAGE gel which was run at 120 V for 2 h and then stained with Coomassie Brilliant Blue.

Assembly State of CadC. Wild-type CadC was subjected to analytical equilibrium sedimentation ultracentrifugation at 35 000 rpm over a range of 10−40 μM CadC monomer under conditions of pH and temperature (pH 7.0, 25.0 °C) identical to those of the metal binding and DNA binding experiments presented below. Representative runs are shown in Figure 2 for 40 μM apo-CadC (panel A) and 40 μM Cd_1-CadC (panel B) under these conditions with 0.20 M NaCl

[2] L. Busenlehner, J. Apuy, and D. P. Giedroc, manuscript in preparation.

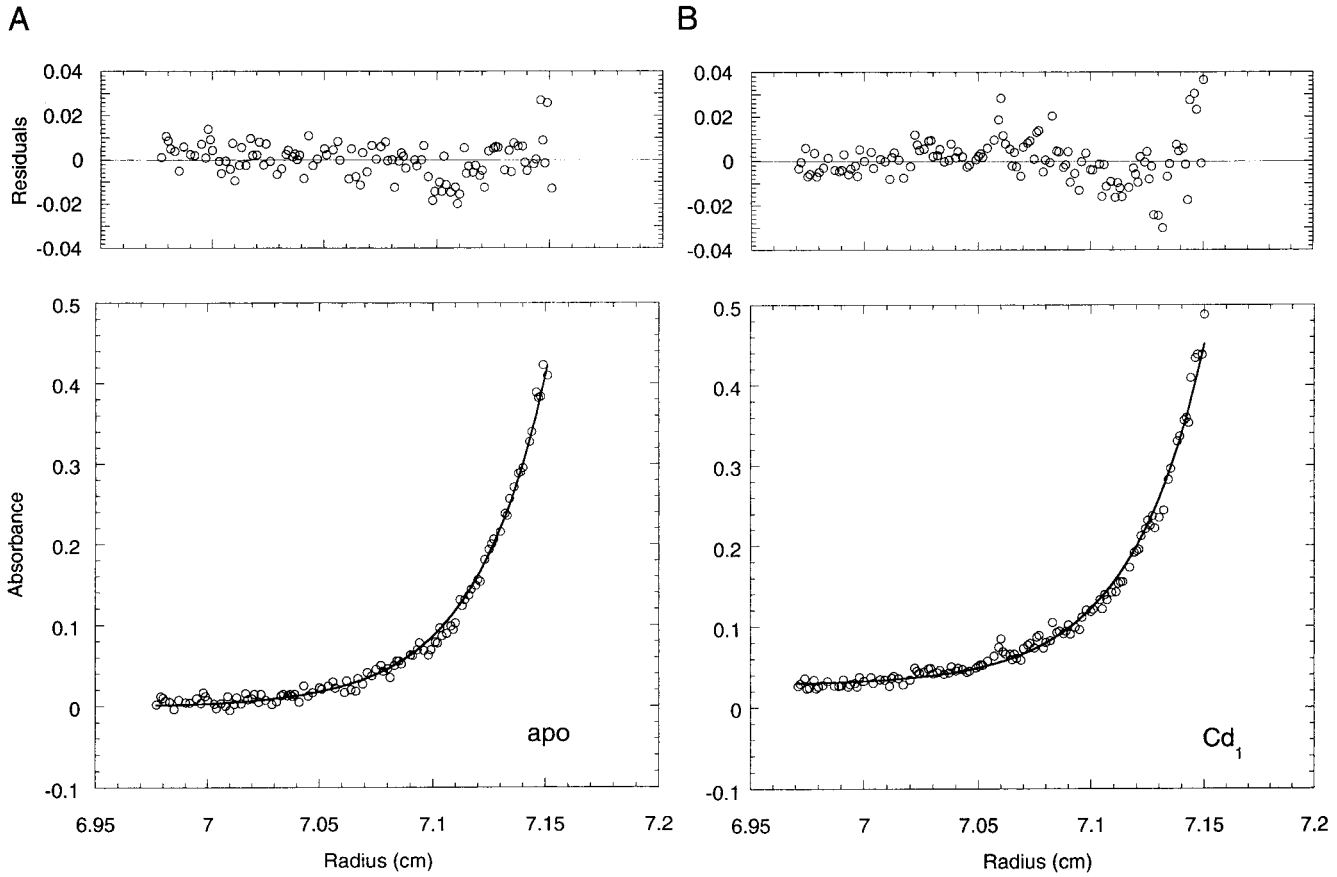

FIGURE 2: Analytical sedimentation equilibrium ultracentrifugation of apo- and Cd_1-CadC. All ultracentrifugation runs were performed at 25 °C with a rotor speed of 35 000 rpm. The fits for the data used a partial specific volume (ν) of 0.724 mL/g and a buffer density (ρ) of 1.006 g/mL. (A) Conditions: 5 mM MES, 0.2 M NaCl, 2 mM DTT, 1 mM EDTA, pH 7.0. The open circles are the data collected for 40 μM metal-free CadC with the solid line representing the best-fit curve for a single ideal species using the Microcal Origin program. The fitted parameter for the molecular mass was calculated to be 29 483 g/mol (predicted molecular mass for a dimer, 27 558 g/mol). (B) Conditions: 5 mM MES, 0.2 M NaCl, 2 mM DTT, pH 7.0. Shown are the data collected for 40 μM CadC with 1 equiv of Cd(II). The solid line corresponds to the best-fit curve for an ideal species. The fitted parameter for the molecular mass was determined to be 28 641 g/mol (predicted molecular mass for a homodimer is 27 558 g/mol).

added. The solid line through each set of experimental data is a fit to a single ideal species model with a fitted molecular mass of 29 483 and 28 641 Da, respectively (Table 2). The expected molecular mass of apo-CadC is 13 779 Da for a monomer, and 27 558 Da for a homodimeric species. Thus, these data are most consistent with CadC forming a predominantly dimeric species under these solution conditions, fully consistent with results from size exclusion chromatography (*10*). Multiple runs collected over a range of [CadC] reveal an average molecular mass of 27 962 (±907) daltons, fully consistent with a homodimeric assembly state in the absence and presence of bound Cd(II) (Table 2).

Each set of equilibrium data was also fit to a monomer−dimer equilibrium model with the monomeric molecular weight and dimerization equilibrium constant, K_{dimer}, fitted parameters (Table 2). Although the goodness-of-fit value (χ^2) is slightly worse in these fits, the residuals can still be described as small and nonrandom (data not shown). The average fitted monomer molecular mass is 13 754 (±154) Da, identical to that expected, with $K_{dimer} = 3.0\ (\pm 2.0) \times 10^6\ M^{-1}$ over all six experiments. Although K_{dimer} in the presence of bound Cd(II) is consistently smaller than that determined for the apo-CadC, the effect is small (within a factor of 2−3); this suggests that the monomer−dimer equilibrium is not strongly linked to metal binding in this system (*26*). This finding is in apparent contrast to a previous report with SmtB (*27*).

Absorption Spectroscopy of Metal Binding by Dimeric Apo-CadC. Shown in Figure 3 are the results of a representative anaerobic Cd(II) binding titration of apo-CadC, with full ultraviolet absorption spectra shown in panel A and the corrected absorbance at 240 nm plotted as a function of Cd(II)/CadC monomer molar ratio in panel B. Formation of the Cd(II)−CadC complex results in a single strong absorption envelope with a maximum absorption at ≈240 nm and a molar absorptivity of $\epsilon_{240} \approx 25\,000\ M_{Cd}^{-1}\ cm^{-1}$ (Figure 3A, inset). This intense absorption is assignable to $S^- \rightarrow Cd(II)$ ligand-to-metal charge transfer (LMCT) transitions and, given a $\epsilon_{248} \approx 5500-6000\ M^{-1}\ cm^{-1}$ per Cd−S bond (*28*, *29*) is most consistent with four cysteine ligands per Cd(II) ion in wild-type CadC. Figure 3B reveals the binding of Cd(II) by wild-type CadC occurs with a stoichiometry of ≈0.7 Cd(II) per total CadC monomer, at least as monitored by optical spectroscopy. Any Cd(II) sites which lack appreciable LMCT absorption would not be detected by this experiment. This result is most consistent with a model in which each CadC monomer within dimeric CadC harbors a single tetrathiolate Cd(II) binding site, with ≈30% of the monomers inactive in Cd(II) binding due perhaps to the

Table 2: CadC Sedimentation Equilibrium Ultracentrifugation Data Analysis

sample	molecular mass (g/mol)	K_{dimer} (M^{-1})[a]	χ^{2} [b]
10 μM apo-CadC[c]			
single, ideal[e]	27715	–	8.29×10^{-5}
dissociable dimer[f]	13790	7.0 ($\pm$0.4) $\times 10^{6}$	9.03×10^{-5}
10 μM Cd_1-CadC[d]			
single, ideal	27283	–	1.00×10^{-4}
dissociable dimer	13805	2.9 ($\pm$0.1) $\times 10^{6}$	1.37×10^{-4}
20 μM apo-CadC[c]			
single, ideal	27403	–	7.03×10^{-5}
dissociable dimer	13647	2.4 ($\pm$0.6) $\times 10^{6}$	1.09×10^{-4}
20 μM Cd_1-CadC[d]			
single, ideal	27250	–	1.04×10^{-4}
dissociable dimer	13502	1.8 ($\pm$0.1) $\times 10^{6}$	1.11×10^{-4}
40 μM apo-CadC[c]			
single, ideal	29483	–	6.33×10^{-5}
dissociable dimer	13923	2.5 ($\pm$0.3) $\times 10^{6}$	1.00×10^{-4}
40 μM Cd_1-CadC[d]			
single, ideal	28641	–	1.02×10^{-4}
dissociable dimer	13861	1.9 ($\pm$0.1) $\times 10^{6}$	1.46×10^{-4}

[a] The association constant as estimated from a best-fit curve using a monomer–dimer equilibrium model (model 2). [b] $\chi^2 = \{\sum_{i=1 \text{ to } n}[f(X_i - Y_i)]^2\}/(N - n)$, where N is the number of observations, n is the number of fitting parameters, $f(\ )$ is the fitting function, X_i and Y_i are data points, and $N - n$ equals the degrees of freedom. [c] Conditions: 5 mM MES, 0.20 M NaCl, 2 mM DTT, 1 mM EDTA, pH 7.0; 25 °C. [d] Conditions: 5 mM MES, 0.20 M NaCl, pH 7.0; 25 °C. [e] Model 1 fits the data to a single, ideal species (see Materials and Methods) with an expected dimer molecular mass of 27 558 g/mol. [f] Model 2 fits the data to a reversible associating system assuming a monomer–dimer equilibrium. The expected monomer molecular mass is 13 779 g/mol (see Materials and Methods).

involvement of metal binding cysteines in formation of a disulfide bond(s) (vida supra). The solid line through the experimental data is a fit to a 1:1 metal binding model; since the binding isotherm is essentially stoichiometric, only a lower limit for K_{Cd} ($\geq 1 \times 10^{7}$ M^{-1}) can be obtained from this experiment. When essentially the same titration is carried out in the presence of 92 μM EDTA, a satisfactory estimate for K_{Cd} can be obtained since EDTA can be used to buffer very low concentrations of free Cd(II), given the conditional stability constant for Cd-EDTA, $K' = 3.2 \times 10^{12}$ M^{-1}, under these conditions (*22*, *23*). A representative titration is shown in Figure 3C. K_{Cd} was determined to be 4.3 ($\pm$1.8) $\times 10^{12}$ M^{-1} from two separate experiments, indicative of very high affinity binding of Cd(II) by apo-CadC.

Figure 4 shows the results of a representative anaerobic titration of the same preparation of apo-CadC with Pb(II) under essentially the same solution conditions. As above, full absorption spectra are shown in panel A, with the binding isotherm shown in panel B. These spectra reveal two intense absorption features: a long-wavelength absorption band with a maximum at 350 nm ($\epsilon_{350} \approx 4000$ M^{-1} cm^{-1}) and a significantly more intense shorter absorption band with an absorption maximum at 240 nm ($\epsilon_{350} \approx 44\,000$ M^{-1} cm^{-1}). Some spectra also exhibit a shoulder at ≈310 nm. Although there are very few published Pb(II)–protein absorption spectra in the literature, previous studies of Pb(II)–peptide complexes would attribute both transitions in Pb(II)-substituted CadC to $S^{-} \rightarrow$Pb(II) LMCT transitions, largely on the basis of their strong intensity and the fact that Pb(II), like Cd(II), has a completely filled *d*-shell (*21*). The molar absorptivity and energy of the absorption band at 350 nm

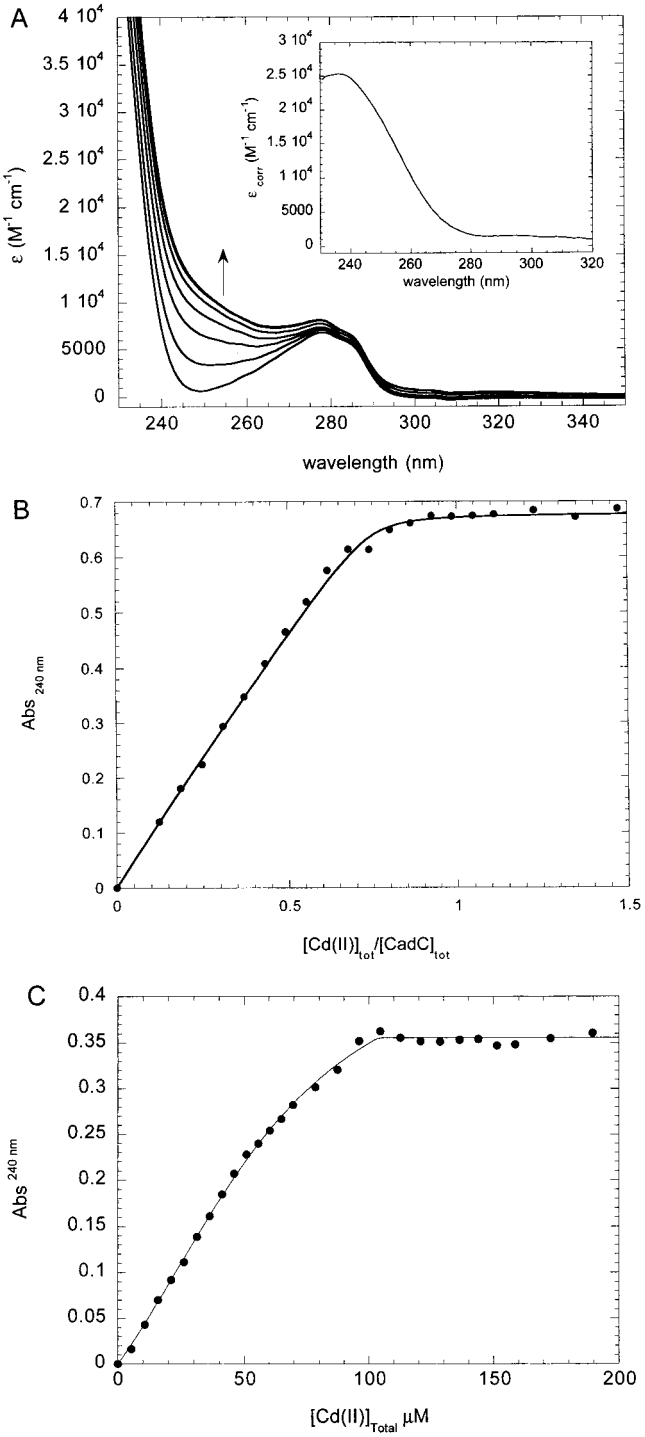

FIGURE 3: Cd(II) titration of CadC. (A) Corrected optical absorption spectrum of 29.1 μM CadC titrated anaerobically with increasing concentrations of Cd(II). Conditions: 5 mM MES, 0.20 M NaCl, pH 7.0, 25 °C. Inset: Apo-subtracted difference spectrum of Cd(II)-saturated CadC expressed per mole of Cd(II) bound reveals $\epsilon_{240} \approx$ 25 000 M^{-1} cm^{-1}. (B) Cd(II) binding isotherm generated from the optical spectrum of a titration of 36.4 μM CadC. The solid curve represents the fit to a 1:1 binding model with $K_{Cd} = 1.3$ ($\pm$0.6) $\times$ 10^{7} M^{-1} (a lower limit) and active [CadC monomer] = 25.4 ($\pm$0.2) μM. (C) Cd-EDTA competition binding isotherm in which 12.7 μM active CadC monomer was titrated with Cd(II) in the presence of 92 μM EDTA. The solid line represents a nonlinear least-squares fit using DynaFit (*20*) to a cooperative binding model assuming two identical sites (one per monomer) characterized by an affinity K_{int} and a cooperativity ω with K_{dimer} fixed at 3×10^{6} M^{-1}. K_{Cd}, derived from $K_{Cd} = \sqrt{K_{int} \cdot \omega}$ (*15*), was determined to be 4.3 ($\pm$1.8) $\times$ 10^{12} M^{-1} from two experiments.

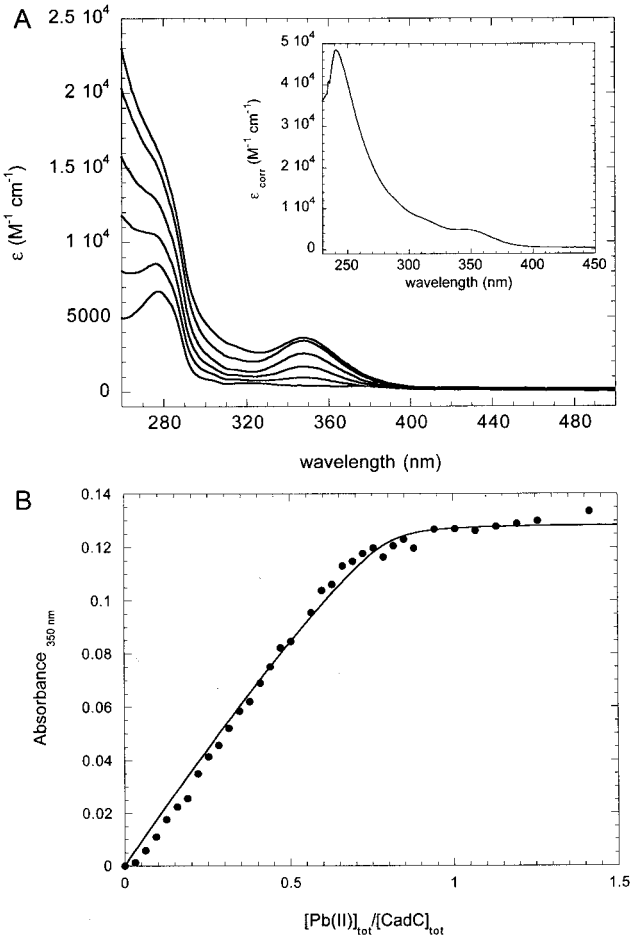

FIGURE 4: Pb(II) titration of CadC. (A) Corrected optical absorption spectrum of 39.4 μM CadC titrated with increasing concentrations of Pb(II) in an anaerobic environment. Conditions: 10 mM Bis-Tris, 0.20 M NaCl, pH 7.0, 25 °C. Inset: Apoprotein-subtracted difference spectrum of Pb(II)-saturated CadC expressed per mole of Pb(II) bound reveals $\epsilon_{350} \approx 4000$ M^{-1} cm^{-1}. (B) Pb(II) binding isotherm generated from the optical spectrum. The solid curve represents the fit to a 1:1 binding model with $K_{Pb} = 1.1$ ($\pm$1.0) $\times$ 10^7 M^{-1} (a lower limit) and active [CadC monomer] = 27.2 ($\pm$0.5) μM.

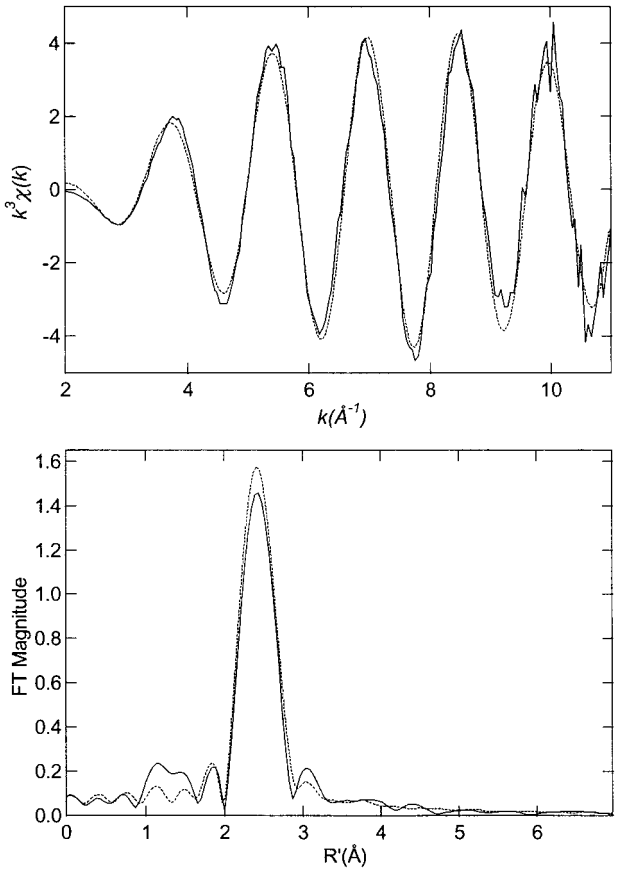

FIGURE 5: X-ray absorption spectra (top) and Fourier transforms (bottom; k = 2−11) of Cd(II)-CadC (solid) and the calculated spectra for Cd-S_4 (dashed; fit 3, Table 3). Conditions: 50 mM MES, 0.40 M NaCl, 20% glycerol, pH 7.0.

Table 3: Curve-Fitting Results for Cd EXAFS of CadC[a]

sample filename (k range) $\Delta k^3\chi$	fit	shell	R_{as} (Å)	σ_{as}^2 (Å^2)	f' [b]
wt CadC + Cd	1	Cd−S_3	2.53	0.0042	0.054
CDC0A (2−11 Å^{-1})	2	Cd−S_3	2.54	0.0023	0.047
$\Delta k^3\chi$ = 9.03		Cd−O	2.25	0.0080	
	3	Cd−S_4	2.53	0.0042	0.046
	4	Cd−S_5	2.54	0.0058	0.054

[a] Group is the chemical unit defined for the multiple scattering calculation. R_{as} is the metal−scatterer distance. σ_{as}^2 is a mean square deviation in R_{as}. [b] f' is a normalized error (chi-squared): $f' = \{\sum_{\times c1}[k^3(\chi_i^{obs} - \chi_i^{calc})]^2/N\}^{1/2}/[(k^3\chi^{obs})_{max} - (k^3\chi_i^{obs})_{min}]$.

are most consistent with three or four, but not two, thiolate ligands forming coordination bonds to the Pb(II) (*21*). Consistent with the Cd(II) titration above, the stoichiometry of Pb(II) binding is ≈0.7 (Figure 4B), with a K_{Pb} in excess of 10^7 M^{-1}. Pb(II) and Cd(II) appear to bind to overlapping sites on CadC since the addition of stoichiometric Cd(II) to the Pb(II)−CadC complex results in complete bleaching of the 350 nm lead−thiolate absorption band (data not shown).

Cd K-edge X-ray Absorption Spectroscopy. Cd K-edge X-ray absorption spectroscopic analysis of Cd(II)-CadC indicates a coordination environment consisting of primarily sulfur scatterers at 2.53 Å (Figure 5). There is a significant reduction in the goodness-of-fit value (f') in the fit that includes four sulfur atoms when compared with fits that include either three or five sulfurs (cf. fit 3 with fits 1 and 4; Table 3). A similar reduction in f' is observed when the EXAFS are fit assuming a coordination environment of three sulfurs and one oxygen atom (fit 2, Table 3). However, the Debye−Waller factor value for the oxygen shell is significantly higher than would be expected a priori for a shell containing a single oxygen atom (more reasonable values would be 0.0015−0.0040 Å^2). Thus, although the EXAFS data cannot unambiguously eliminate a Cd(II)−S_3O coordination environment, the data are most consistent with coordination of the Cd(II) ion by four sulfur ligands. These data have been reproduced on three samples from two different laboratories (D. P. Giedroc and B. P. Rosen).

^{113}Cd NMR Spectroscopy of ^{113}Cd(II)-Substituted CadC. The ^{113}Cd chemical shift (δ) of the Cd(II) complexes formed by metalloproteins is extremely sensitive to the nature of the first shell of ligands around the Cd(II) ion (*16*). Mononuclear tetrathiolate (S_4) sites associated with structural Zn(II) sites in zinc metalloproteins are typically characterized by δ = 700−750 ppm [downfield from 0.1 M $Cd(ClO_4)_2$]. S_3(N,O) resonate slightly further upfield, in the range between ≈630 and 660 ppm, with a nitrogen ligand usually moderately more deshielding than an oxygen ligand. How-

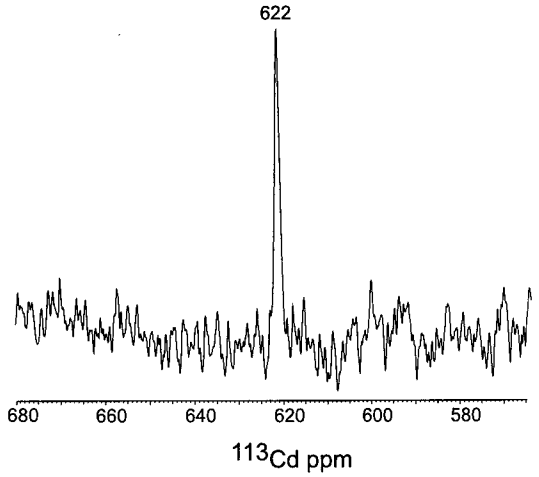

FIGURE 6: ^{113}Cd NMR spectrum of ^{113}Cd-substituted CadC. Conditions: 5 mM d^{18} HEPES, 0.35 M NaCl, 10% D_2O, pH 7.0, 25.0 °C. Chemical shift is reported relative to 0.10 M $Cd(ClO_4)_2$. 74 880 transients were acquired, and an exponential line broadening function of 50 Hz was applied prior to Fourier transformation.

ever, multinuclear S_4 sites, in which some subsets of cysteine ligands in an S_4 complex donate two coordination bonds to each of two Cd(II) ions, are characterized by ^{113}Cd δ upfield of a mononuclear S_4 site, in the 610−700 ppm range (*16*). Figure 6 shows that the 110.9 MHz ^{113}Cd NMR spectrum of ^{113}Cd-complexed CadC is characterized by $\delta = 622$ ppm, a chemical shift consistent with S_3(N,O) or an unusual upfield-shifted S_4 coordination complex (see Discussion).

Allosteric Regulation of cad O/P Binding of CadC by Cd(II) and Pb(II). Previously published gel mobility shift experiments suggested that the addition of exogenously added Cd(II), Pb(II), or Bi(III) to preformed apo-CadC−DNA complexes resulted in some dissociation of the DNA-bound CadC (*11*). The results of assays in which CadC protects the *cad* O/P from restriction enzyme digestion also show that Pb(II), Cd(II), or Zn(II) produces dissociation of the repressor−DNA complex (*10*). However, the stoichiometry and affinity of CadC for its specific binding site, as well as the mode of metalloregulation, could not be determined from those experiments. We designed a fluorescein-labeled 34 base pair DNA oligonucleotide into which was incorporated the region of the *cad* operator/promoter (O/P) region that is strongly footprinted by bound CadC (*11*). This includes the imperfect 12-2-12 inverted repeat. CadC binding was then monitored by measuring the increase in anisotropy of the fluorescein fluorescence upon formation of the protein−DNA complex.

Figure 7 shows representative binding experiments carried out with apo-CadC under solution conditions of relatively high monovalent salt concentration (pH 7.0, 0.40 M NaCl, 25.0 °C), but which are otherwise identical to those of the metal binding and analytical ultracentrifugation experiments presented above. High salt was found to be necessary to minimize the formation of higher order CadC−DNA complexes, with the limiting dimeric $(CadC)_2$−DNA complex the dominant complex formed, even at excess [CadC] (data not shown). The fitted parameters resolved from multiple experiments are collated in Table 2. The solid line through each set of experimental data in Figure 7 represents a fit to

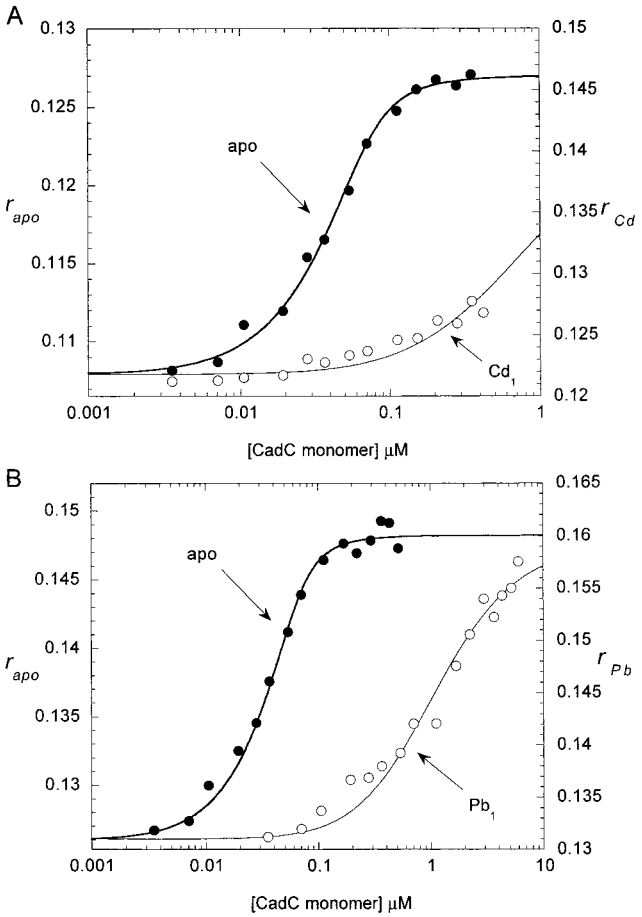

FIGURE 7: Fluorescence anisotropy of CadC binding to *cad* O/P DNA. (A) Shown is the anisotropy-based binding isotherm obtained upon titration of the 5′-fluorescein-labeled *cad* O/P with apo-CadC (●) and Cd_1-CadC (○) at 25 °C in 5 mM MES, 0.20 M NaCl, 1 mM DTT, 50 μM EDTA (EDTA not present in the Cd-CadC titration), pH 7.0. The solid line through the points represents a fit of the anisotropy data to a dissociable dimer model assuming a 1:1 dimer/DNA complex with a dimerization constant fixed at 3×10^6 M^{-1}. For the apo-CadC titration, $K_{app} = 1.0\ (\pm 0.1) \times 10^9$ M^{-1} while $K_{app} = 4.9\ (\pm 0.6) \times 10^6$ M^{-1} for the Cd_1-CadC titration. (B) Shown is the binding isotherm obtained upon titration of the 5′-fluorescein-labeled *cad* O/P with apo-CadC (●) and Pb_1-CadC (○) in 10 mM Bis-Tris, 0.20 M NaCl, 1 mM DTT, 50 μM EDTA (EDTA not present in the Pb-CadC titration), pH 7.0, and 25 °C. The solid line through the experimental data represents a best fit of the anisotropy data to a dissociable dimer model that assumes a 1:1 dimer/DNA complex with a dimerization constant fixed at 3×10^6 M^{-1}. For the apo-CadC titration, $K_a = 1.3\ (\pm 0.08) \times 10^9$ M^{-1} while $K_a = 3.4\ (\pm 0.6) \times 10^6$ M^{-1} for the Pb_1-CadC titration.

a model that describes the binding of a dissociable CadC dimer to a single site on the DNA:

$$2\text{CadC} \overset{K_{dimer}}{\Longleftrightarrow} (\text{CadC})_2 + \text{D} \overset{K_a}{\leftrightarrow} (\text{CadC})_2\cdot\text{D}$$

In these fits, K_{dimer} was constrained to a value of 3.0×10^6 M^{-1}, the average value estimated by analytical ultracentrifugation (Table 2), with the fits optimized for K_a and a value for the anisotropy (r_{max}) of the $(CadC)_2$−DNA complex. A linear correlation between a change in r_{obs} and the fractional saturation of the DNA was assumed in this analysis. The data reveal that dimeric CadC forms a very tight complex with its DNA binding site with $K_a = 1.1\ (\pm 0.3) \times 10^9$ M^{-1}, indicating strong linkage to the monomer−dimer equilibrium

Table 4: Summary of the Affinities of Apo- and Metalated CadCs for the *cad* O/P Oligonucleotide

CadC	K_a (M^{-1})[d]	fold decrease relative to apo
apo[a]	1.1 (±0.2) × 10^9	–
Cd_1[b]	4.9 (±0.6) × 10^6	230
Pb_1[c]	3.4 (±0.6) × 10^6	340

[a] Conditions: 5 mM MES or 10 mM Bis-Tris, 0.40 M NaCl, 50 μM EDTA, 1 mM DTT, pH 7.0, 25 °C. [b] Conditions: 5 mM MES, 0.40 M NaCl, 1 mM DTT, pH 7.0, 25.0 °C. [c] Conditions: 10 mM Bis-Tris, 0.40 M NaCl, 1 mM DTT, pH 7.0, 25.0 °C. [d] Binding isotherms were fit as described under Materials and Methods using a dissociable dimer model with K_{dimer} fixed at 3 × 10^6 M^{-1}.

under these conditions. In striking contrast, the addition of a single equivalent of bound Cd(II) (panel A) or Pb(II) (panel B) per CadC monomer results in strong negative regulation of *cad* O/P binding, with K_a reduced by 230−340-fold relative to that of apo-CadC (Table 4).

DISCUSSION

In this report, we have determined the quaternary structure and the stoichiometry, affinity, and coordination structure of the metalloregulatory Cd(II)/Pb(II) site of *S. aureus* pI258 CadC. CadC is predominantly homodimeric at protein concentrations in excess of the low micromolar range at neutral pH and 25 °C. The spectroscopic data are consistent with a model in which each subunit of homodimeric CadC contributes ligands to each of two Cd(II) or Pb(II) ions bound to the dimer. Cd(II) and Pb(II) appear to bind with extremely high affinity, with K_{Cd} estimated to be in the 10^{12} M^{-1} range as determined from EDTA competition experiments. Approximately stoichiometric Pb(II) gives rise to complete displacement of the Cd(II) (data not shown), revealing that Cd(II) and Pb(II) share some or all of the metal ligands; furthermore, these data suggest that Pb(II) binds with an affinity comparable to that of Cd(II).

The optical absorption and X-ray absorption spectra obtained for the Cd(II)-substituted CadC are most consistent with a coordination model in which four of the five cysteines in CadC donate ligands to the Cd(II) ion. For example, the tetrathiolate Cd(II) complexes of *D. gigas* rubredoxin (*29*) and coliphage 186 B protein (*28*) are characterized by ϵ_{248} = 24 000 M_{Cd}^{-1} cm^{-1}, similar to that obtained for Cd(II)-substituted CadC; in contrast, a well-characterized S_3N complex gives $\epsilon_{248} \approx 15\,000$ M^{-1} cm^{-1} (*30*). By analogy with the crystallographic structure of metal-free *Synechococcus* SmtB (*12*), two Cys residues in CadC are present in the N-terminal unstructured region, Cys7 and Cys11, while two more are present in the putative metal binding helix within the EL**C**V**C**D sequence, Cys58 and Cys60. Three of the four Cys are invariant (Cys7, Cys58, and Cys60), with Cys11 conserved, but not invariant (*10*). A fifth Cys residue, Cys52, is not conserved in other CadC proteins or in other members of the ArsR superfamily. This sequence conservation is therefore most consistent with a model in which Cys7 and Cys11 from the N-terminal arm, and Cys58 and Cys60 contribute ligands to the Cd(II) ion. This is also consistent with the spectroscopic characterization of cysteine mutant CadC proteins.[2] Interestingly, recent functional results demonstrate that substitution of Cys7, Cys58, or Cys60 but not Cys11 or Cys52 produces loss of sensing of Pb(II), Cd(II), or Zn(II), both in vivo and in vitro (*10*). Thus, while Cys11 is not required, it may still contribute a Cd(II)−S coordination bond. In the homologous ArsR repressor, Sb(III) and As(III) are bound three-coordinately to Cys32, Cys34, and Cys37 (*31*). However, only Cys32 and Cys34 are required since substitution of Cys37 has no effect on biological activity.

It is unknown if Cys7 and Cys11 are derived from different or the same monomer subunit as Cys58 and Cys60. It is clear, however, that either one of the N-terminal Cys residues is close enough to Cys58 or Cys60 to form a disulfide bond, apparently concomitant with inactivation of Cd(II) binding to that site in the dimer. The fact that the appearance of this cross-linked fragment is at least partially correlated with the presence of a cross-linked dimer on denaturing gels is consistent with at least some fraction of these cross-links being intersubunit.[3]

In contrast to the conclusions about the Cd(II) coordination environment drawn from optical and X-ray absorption spectroscopy, the chemical shift obtained for ^{113}Cd-CadC (δ = 622 ppm) is *not* strongly consistent with a typical mononuclear S_4 complex (*16*). Rather, this chemical shift is more consistent with a S_3(N,O) environment or a "polynuclear-like" S_4 complex, in which the full deshielding effect of one or more of the Cys residues in a tetrathiolate complex is not fully experienced at the ^{113}Cd nucleus. The chemical shifts of a number of structurally well-characterized S_3N ^{113}Cd complexes have been found to range from ≈630 to 660 ppm (for a review, see refs *16*, *30*, *32*−*35*). One exception to this is a ^{113}Cd-substituted S_3O site in a mutant form of HIV-1 integrase, which is reported to be characterized by δ = 538 ppm (*36*). In contrast, nearly all mononuclear S_4 sites resonate at 700 ppm or further downfield (*16*, *37*). The most upfield-shifted mononuclear S_4 site thus far reported is δ = 684 ppm from the ^{113}Cd-substituted catalytic zinc site of *E. coli* Ada, which repairs methyl phosphotriesters via irreversible methyl transfer to one of the liganding cysteines (*38*).

On the other hand, S_4 sites containing bridging or shared thiolate ligands, like that which is present in mammalian metallothioneins (*39*, *40*) and binuclear cluster transcription factors from the yeast Gal4 family (*41*−*43*), are characterized by ^{113}Cd δ which range between ≈610 and 710 ppm. The most upfield-shifted of these S_4 sites range from δ = 611 to δ = 632 ppm in mammalian metallothioneins; these complexes are unique among multinuclear sites in that three of the four thiolate ligands bridge two ^{113}Cd ions (*44*). Finally, there is only one purported trigonal S_3 ^{113}Cd complex reported thus far; this de novo designed site gives δ = 572 ppm (*45*).

^{113}Cd NMR spectroscopy is therefore most compatible with either an S_3N, S_3O, or unusual S_4 coordination environment in CadC.[4] An S_3N site seems unlikely since there are no

[3] We have recently shown that apo-C121S SmtB can reversibly form an intersubunit disulfide bond between Cys14 and Cys61 on different monomers, which are analogous to Cys11 and Cys58, respectively, in the wild-type CadC pI258 amino acid sequence (X. Chen, M. VanZile, and D. P. Giedroc, unpublished observations).

[4] Attempted applications of a variety of ^{1}H{^{113}Cd} heteronuclear multiple quantum correlation (HMQC) or spin−echo difference experiments (*53*, *54*) on ^{113}Cd-substituted CadC have thus far been unsuccessful, due presumably to a combination of weak ^{1}H−^{113}Cd three-bond couplings and very short T_2's associated with this 27.5 kDa dimer (L. S. Busenlehner and D. P. Giedroc, unpublished observations).

obvious candidates for a conserved imidazole ligand to create an S_3N site in CadC (*10*). Another possible interpretation of a ^{113}Cd δ of 622 ppm is a S_3S_{Met} first shell. However as with histidine, there are no strongly conserved Met residues in the N-terminal domain or in the $E^{56}LCVCD^{61}$ region (*10*); in addition, a Cd−thioether bond length would likely be much longer than a Cd−thiolate bond, an expectation incompatible with the EXAFS data. As for an S_3O complex, there are a number of conserved carboxylate residues, including Glu8, Glu14, and Glu15 in the N-terminal arm, in addition to Glu56 and Asp61 in the $E^{56}LCVCD^{61}$ putative metal binding region; any one of these could combine with strictly conserved Cys7, Cys58, and Cys60 to create such a site. Interestingly, only Glu14 and Glu15 are conserved in CadCs that have been shown to specifically sense Cd(II), while the $\underline{E}^{56}LCVC\underline{D}^{61}$-derived carboxylate residues are common to all ArsR family members. Although the EXAFS cannot conclusively rule out a Cd(II)−S_3O coordination environment, one would expect a significantly lower Debye−Waller value for the Cd−O shell than is experimentally observed (Table 3), indicating that the coordination environment is composed of primarily sulfur scatterers.

An alternative interpretation of the ^{113}Cd chemical shift is that a nonthiolate ligand is derived from the solvent, which in this case would implicate either a H_2O molecule or a Cl^- ion, the latter of which is a strong possibility since both the EXAFS and ^{113}Cd NMR experiments were carried out in 0.35−0.40 M NaCl required to solubilize CadC to ≈1 mM for these experiments. A bound Cl^- ion would be indistinguishable from a thiolate ligand in Cd(II) EXAFS. Cl^- will also be more deshielding than a solvent H_2O ligand, which would tend to move the ^{113}Cd resonance line to larger δ relative to an S_3O site (*46*). Unfortunately, the magnitude of this effect is difficult to predict a priori but can be as much as 30 ppm (*16, 46*). Attempts to exchange the Cl^- with Br^-, a more potent scatterer in an EXAFS experiment, or F^-, which should be less deshielding then Cl^- in an ^{113}Cd NMR experiment, are underway. In the absence of these data, we currently favor the unusual S_4 interpretation involving Cys7, Cys11, Cys58, and Cys60, particularly when taken together with the optical absorption and EXAFS analysis of wild-type CadC and Cys substitution mutants of CadC.[2] A significantly less deshielded ^{113}Cd nucleus might result from one of the Cd−thiolate bonds being slightly longer (if so, this is not readily apparent from the EXAFS *average* Cd−S distance), or from a nonoptimal C−S−^{113}Cd dihedral angle derived from a site which deviates strongly from tetrahedral symmetry; this would be expected to significantly alter the shielding tensor, and/or reduce the covalent character of one or more of the ^{113}Cd−S coordination bonds in CadC (*47, 48*).

Previous studies which examined the metal specificity of the metalloregulation of the *cad* O/P (*10, 11*) suggest that CadC binds Pb(II) ions. Our results from optical absorption spectroscopy provide direct evidence for this; furthermore, the stoichiometry and efficient competition by Cd(II) reveal that the Cd(II) and Pb(II) sites at least partially overlap in CadC. This is consistent with the observation that cysteine-substituted CadC mutants have nearly equivalent reduction in sensing of Pb(II), Cd(II), and Zn(II) (*10*). Unfortunately, unlike the case with Cd(II), it is not entirely clear how the UV−Vis absorption spectrum reports on the nature and number of first-shell ligands. Indeed, only one report has investigated the spectroscopic properties of protein−Pb(II) chelates; this study examined the 1:1 Pb(II) complexes formed by peptide models of native zinc binding S_4, S_3N, and S_2N_2 sites (*21*). Although the number of Pb(II)−S bonds was not determined in these peptide complexes, Pb(II) complexes formed by the S_4 and two different S_3N models could not be distinguished from one another and were characterized by two prominent lead−thiolate LMCT bands positioned at 335 nm (ϵ = 4000 M^{-1} cm^{-1}) and 260 nm (ϵ = 16 000 M^{-1} cm^{-1}). In contrast, the Pb(II) complex formed by the S_2N_2 peptide gave rise to a pronounced blue shift in the long-wavelength transition to 310 nm, with less molar absorptivity in the 260 nm region. Comparison of the spectrum of Pb(II)-substituted CadC with these published spectra is fully consistent with three or four thiolate ligands, but not two. It is important to point out, however, that Pb(II) has been shown to form very stable three-coordinate complexes with three sulfur donor ligands in the catalytic S_3O Zn(II) site in 5-aminolevulinate dehydratase (ALAD; porphobilinogen synthase) (*49*) and in the ALAD model ligand tris(mercaptoaryl-imidazoyl)borate (*50*). In these complexes, the three S^- donors form the base of trigonal pyramidyl coordination structure, with the stereochemically active 6s lone pair of electrons thought to occupy the apical position of the Pb(II) coordination complex (*51*). Interestingly, Pb(II) is bound to ALAD through a Cys-X-Cys...Cys sequence (*49*), which is not unlike the Cys^7 (or Cys^{11})...Cys^{58}-Val^{59}-Cys^{60} sequence in CadC. Spectroscopic characterization of cysteine substitution mutants of CadC will be capable of discriminating between these two Pb(II) coordination models.[2]

Finally, we show here that these structurally characterized Cd(II) and Pb(II) binding sites in CadC are necessary and sufficient for strong negative allosteric regulation of the *cad* O/P binding activity of metal-free, dimeric apo-CadC. This is consistent with a model in which the direct binding of regulatory metals by CadC results in a significant reduction in the DNA binding affinity, that allows access by RNA polymerase to the promoter, and subsequent derepression of transcription (*10, 11*). Metal-free CadC forms a high-affinity complex with a DNA oligonucleotide which harbors a specific binding site for CadC, as defined by previous functional and DNase I footprinting experiments (*11*). Under the solution conditions used here (25 °C, pH 7.0, 0.40 M NaCl), the DNA binding isotherms are well described by a model in which the monomer−dimer equilibrium of apo-CadC is linked to specific DNA binding by the homodimer. Analysis of binding isotherms in a way that assumes a nondissociable CadC dimer misses the experimental data at both the low and high concentrations of total monomer; i.e., the experimental binding curve is too steep, a result consistent with linkage to protein assembly (data not shown) (*52*). When K_{dimer} determined independently from sedimentation equilibrium experiments is used as a fixed parameter in nonlinear least-squares fits to the experimental data, satisfactory fits to the data characterized by random residuals are obtained with K_a readily resolved (Table 4). Since the Cd_1 and Pb_1 forms of the protein bind much more weakly to the DNA, there is considerably less linkage to the monomer−dimer equilibrium with these forms because significant dimer is present in solution under conditions of measurable complex

formation with the DNA. In any case, the binding of Cd(II) and Pb(II) reduces the intrinsic affinity of dimeric CadC for the *cad* O/P site significantly and to essentially the same extent, by as much as ≈300-fold with K_{dimer} fixed at 3.0×10^6 M^{-1}, with a lower limit of ≈50-fold, if one assumes a nondissociable CadC dimer. The precise mechanism of the allosteric regulation by metal ions of the initiation of transcription in this system is the subject of current work.

ACKNOWLEDGMENT

The XAS data were collected at Stanford Synchrotron Radiation Laboratory (SSRL), which is operated by the U.S. Department of Energy, Division of Chemical Sciences. The SSRL Biotechnology Program is supported by the National Institutes of Health, Biomedical Technology Program, Division of Research Resources. We thank Dr. Larry Dangott in the Protein Chemistry Laboratory at Texas A&M University for his determination of the N-terminal sequences of CadC, Mr. Julius Apuy for the MALDI-TOF determination of the molecular weight of recombinant CadC, and Dr. Simon Silver at the University of Illinois at Chicago for his gift of a plasmid encoding the wild-type *S. aureus* pI258 *cadC* gene. We also thank Dr. Victoria DeRose, Department of Chemistry, Texas A&M University, for many helpful suggestions.

REFERENCES

1. Xu, C., and Rosen, B. P. (1999) in *Metals and Genetics* (Sarkar, B., Ed.) p 406, Plenum Press, New York.
2. O'Halloran, T. V. (1993) *Science 261*, 715−725.
3. Rensing, C., Ghosh, M., and Rosen, B. P. (1999) *J. Bacteriol. 181*, 5891−5897.
4. Mitra, B., Gatti, D. L., and Rosen, B. P. (2000) *J. Biol. Chem. 275*, 34009−34012.
5. Shi, W., Wu, J., and Rosen, B. P. (1994) *J. Biol. Chem. 269*, 19826−19829.
6. Nies, D. H., and Brown, N. L. (1998) in *Metal Ions in Gene Regulation* (Silver, S., and Walden, W., Eds.) pp 77−103, Chapman and Hall, New York.
7. Wu, J., and Rosen, B. P. (1991) *Mol. Microbiol. 5*, 1331−1336.
8. Nucifora, G., Chu, L., Misra, T. K., and Silver, S. (1989) *Proc. Natl. Acad. Sci. U.S.A. 86*, 3544−3588.
9. Rensing, C., Sun, Y., Mitra, B., and Rosen, B. P. (1998) *J. Biol. Chem. 273*, 32614−32617.
10. Sun, Y., Wong, M., and Rosen, B. P. (2001) *J. Biol. Chem.* (in press).
11. Endo, G., and Silver, S. (1995) *J. Bacteriol. 177*, 4437−4441.
12. Cook, W. J., Kar, S. R., Taylor, K. B., and Hall, L. M. (1998) *J. Mol. Biol. 275*, 337−346.
13. Morby, A. P., Turner, J. S., Huckle, J. W., and Robinson, N. J. (1993) *Nucleic Acids Res. 21*, 921−925.
14. Daniels, M. J., Turner-Cavet, J. S., Selkirk, R., Sun, H., Parkinson, J. A., Sadler, P. J., and Robinson, N. J. (1998) *J. Biol. Chem. 273*, 22957−22961.
15. VanZile, M. L., Cosper, N. J., Scott, R. A., and Giedroc, D. P. (2000) *Biochemistry 39*, 11818−11829.
16. Gulin, O., Pountney, D. L., and Armitage, I. M. (1998) *Biochem. Cell Biol. 76*, 223−243.
17. Sambrook, J., Fritsch, E. F., and Maniatis, T. (1989) *Molecular Cloning: A Laboratory Manual*, Cold Spring Harbor Laboratory Press, Cold Spring Harbor, NY.
18. Pace, C. N., Vajdos, F., Fee, L., Grimsley, G., and Gray, T. (1995) *Protein Sci. 4*, 2411−2423.
19. Guo, J., and Giedroc, D. P. (1997) *Biochemistry 36*, 730−742.
20. Kuzmic, P. (1996) *Anal. Biochem. 237*, 260−273.
21. Payne, J. C., ter Horst, M. A., and Godwin, H. A. (1999) *J. Am. Chem. Soc. 121*, 6850−6855.
22. Nasir, M. S., Fahrni, C. J., Suhy, D. A., Kolodsick, K. J., Singer, C. P., and O'Halloran, T. V. (1999) *J. Biol. Inorg. Chem. 4*, 775−783.
23. Martell, A. E., and Smith R. M. (1974−1989) *Critical stability constants*, Plenum Press, New York.
24. Scott, R. A. (1985) *Methods Enzymol. 117*, 414−459.
25. Chen, X., Agarwal, A., and Giedroc, D. P. (1998) *Biochemistry 37*, 11152−11161.
26. Laue, T. M., and Stafford, W. F., III. (1999) *Annu. Rev. Biophys. Biomol. Struct. 28*, 75−100.
27. Kar, S. R., Adams, A. C., Lebowitz, J., Taylor, K. B., and Hall, L. M. (1997) *Biochemistry 36*, 15343−15348.
28. Poutney, D. L., Tiwari, R. P., and Egan, J. B. (1997) *Protein Sci. 6*, 892−902.
29. Henehan, C. J., Pountney, D. L., Zerbe, O., and Vasék, M. (1993) *Protein Sci. 2*, 1756−1764.
30. Chen, X., Chu, M., and Giedroc, D. P. (2000) *J. Biol. Inorg. Chem. 5*, 93−101.
31. Shi, W. P., Dong, J., Scott, R. A., and Rosen, B. P. (1996) *J. Biol. Chem. 271*, 9291−9297.
32. Qiu, H., and Giedroc, D. P. (1994) *Biochemistry 33*, 8139−8148.
33. Kosa, J. L., Michelsen, J. W., Louis, H. A., Olsen, J. I., Davis, D. R., Berkerle, M. C., and Winge, D. R. (1994) *Biochemistry 33*, 468−477.
34. South, T. L., Kim, B., and Summers, M. F. (1989) *J. Am. Chem. Soc. 111*, 395−396.
35. Fitzgerald, D. W., and Coleman, J. E. (1991) *Biochemistry 30*, 5195−5201.
36. Cai, M., Huang, Y., Caffrey, M., Zheng, R., Craigie, R., Clore, G. M., and Gronenborn, A. M. (1998) *Protein Sci. 7*, 2669−2674.
37. Pan, T., Freedman, L. P., and Coleman, J. E. (1990) *Biochemistry 29*, 9218−9225.
38. Myers, L. C., Terranova, M. P., Ferentz, A. E., Wagner, G., and Verdine, G. L. (1993) *Science 261*, 1164−1167.
39. Otvos, J. D., and Armitage, I. M. (1980) *Proc. Natl. Acad. Sci. U.S.A. 77*, 7094−7098.
40. Zangger, K., Öz, G., Otvos, J. D., and Armitage, I. M. (1999) *Protein Sci. 8*, 2630−2638.
41. Pan, T., and Coleman, J. E. (1989) *Proc. Natl. Acad. Sci. U.S.A. 86*, 3145−3149.
42. Pan, T., Halvorsen, Y.-D., Dickson, R. C., and Coleman, J. E. (1990) *J. Biol. Chem. 265*, 21427−21429.
43. Anderson, S. F., Steber, C. M., Esposito, R. E., and Coleman, J. E. (1995) *Protein Sci. 4*, 1832−1843.
44. Otvos, J. D., and Armitage, I. M. (1980) *Biochemistry 19*, 4031−4043.
45. Li, X., Suzuki, K., Kanaori, K., Tajima, K., Kashiwada, A., Hiroaki, H., Kohda, D., and Tanaka, T. (2000) *Protein Sci. 9*, 1327−1333.
46. Gettins, P., and Coleman, J. E. (1984) *J. Biol. Chem. 259*, 11036−11040.
47. Marchetti, P. S., Bank, S., Bell, T. W., Kennedy, M. A., and Ellis, P. D. (1989) *J. Am. Chem. Soc. 111*, 2063−2066.
48. Marchetti, P. S., Ellis, P. D., and Bryant, R. G. (1985) *J. Am. Chem. Soc. 107*, 8191−8196.
49. Warren, M. J., Cooper, J. B., Wood, S. P., and Shoolingin-Jordan, P. M. (1998) *Trends Biochem. Sci. 23*, 217−221.
50. Bridgewater, B. M., and Parkin, G. (2000) *J. Am. Chem. Soc. 122*, 7140−7141.
51. Shimoni-Livny, L., Glusker, J. O. P., and Bock, C. W. (1998) *Inorg. Chem. 37*, 1853−1867.
52. Brenowitz, M., Jamison, E., Majumdar, A., and Adhya, S. (1990) *Biochemistry 29*, 3374−3383.
53. Wörgötter, E., Wagner, G., and Wüthrich, K. (1986) *J. Am. Chem. Soc. 108*, 6162−6167.
54. Gardner, K. H., and Coleman, J. E. (1994) *J. Biomol. NMR 4*, 761−774.

BI010006G